TECHNICAL REPORT

ISO/ASTM TR 52952

First edition
2023-06

Additive manufacturing of metals — Feedstock materials — Correlating of rotating drum measurement with powder spreadability in PBF-LB machines

Fabrication additive de métaux — Matières premières — Corrélation de la mesure du tambour rotatif avec la capacité d'étalement de la poudre dans les machines PBF-LB

Reference number
ISO/ASTM TR 52952:2023(E)

ISO copyright office
CP 401 • Ch. de Blandonnet 8
CH-1214 Vernier, Geneva
Phone: +41 22 749 01 11

Email: copyright@iso.org
Website: www.iso.org

ASTM International
100 Barr Harbor Drive, PO Box C700
West Conshohocken, PA 19428-2959, USA
Phone: +610 832 9634
Fax: +610 832 9635
Email: khooper@astm.org
Website: www.astm.org

Published in Switzerland

Contents

Foreword

ISO (the International Organization for Standardization) is a worldwide federation of national standards bodies (ISO member bodies). The work of preparing International Standards is normally carried out through ISO technical committees. Each member body interested in a subject for which a technical committee has been established has the right to be represented on that committee. International organizations, governmental and non-governmental, in liaison with ISO, also take part in the work. ISO collaborates closely with the International Electrotechnical Commission (IEC) on all matters of electrotechnical standardization.

The procedures used to develop this document and those intended for its further maintenance are described in the ISO/IEC Directives, Part 1. In particular, the different approval criteria needed for the different types of ISO documents should be noted. This document was drafted in accordance with the editorial rules of the ISO/IEC Directives, Part 2 (see www.iso.org/directives).

Attention is drawn to the possibility that some of the elements of this document may be the subject of patent rights. ISO shall not be held responsible for identifying any or all such patent rights. Details of any patent rights identified during the development of the document will be in the Introduction and/or on the ISO list of patent declarations received (see www.iso.org/patents).

Any trade name used in this document is information given for the convenience of users and does not constitute an endorsement.

For an explanation of the voluntary nature of standards, the meaning of ISO specific terms and expressions related to conformity assessment, as well as information about ISO's adherence to the World Trade Organization (WTO) principles in the Technical Barriers to Trade (TBT), see www.iso.org/iso/foreword.html.

This document was prepared by Technical Committee ISO/TC 261, *Additive manufacturing*, in cooperation with ASTM Committee F42, *Additive Manufacturing Technologies*, on the basis of a partnership agreement between ISO and ASTM International with the aim to create a common set of ISO/ASTM standards on additive manufacturing, and in collaboration with the European Committee for Standardization (CEN) Technical Committee CEN/TC 438, *Additive manufacturing,* in accordance with the Agreement on technical cooperation between ISO and CEN (Vienna Agreement).

Any feedback or questions on this document should be directed to the user's national standards body. A complete listing of these bodies can be found at www.iso.org/members.html.

Introduction

Granular materials and fine powders are widely used in industrial applications. To support control and optimize processing methods, these materials have to be precisely characterized. Characterization methods are related either to the properties of the grains (granulometry, morphology, chemical composition, etc.) or to the behaviour of the bulk powder (flowability, density, blend stability, electrostatic properties, etc.). The complex behaviours of granular and powder materials have motivated the development of numerous techniques to obtain reproducible and interpretable results. Many industries are concerned in different fields: additive manufacturing, food processing, pharmaceuticals, bulk material handling. This document is focused on Additive Manufacturing (AM).

Metallic powders are widely used in AM processes involving powder bed fusion (PBF-LB/M PBF-EB/M etc.) or binder jetting. During such operations, successive thin layers of powder are deposited with a blade or with a rotating cylinder. Each layer is then fused (most commonly melted) by an energy beam or joined by an adhesive binder to build the parts. The layer thickness defines the vertical resolution of the process; a thin layer leads to a better resolution. In order to obtain a thin layer, the powder is as fine as possible. However, if it is assumed that among the cohesive forces, the Van der Waal forces are predominant, it can be stated that as the grain size decreases, cohesiveness typically increases[25]. This increase in cohesiveness could have an impact on the spreadability of a powder.

The quality of the parts built with AM is thus directly influenced by powder flow properties.

According to ISO/ASTM 52900, spreadability is the ability of a feedstock material to be spread out in layers that fulfil the requirements for the AM process; this includes the ability to form a flat powder-atmosphere interface without waves and irregularities.

Visual observation of layer homogeneity is usually the only way for operators to assess the spreadability of powders during the spreading of new layers. However, linking the powder characteristics to its spreadability during the layer deposition beforehand can provide a more cost-effective way to classify and select the optimal powder and layer deposition speed combinations.

Additive manufacturing of metals — Feedstock materials — Correlating of rotating drum measurement with powder spreadability in PBF-LB machines

1 Scope

This document provides an example of the relation between the characterization of certain macroscopic properties of metallic powders and their spreadability in an PBF-LB/M AM machines.

This relation is based on a new technique combining measurements inside a PBF-LB/M machine and image processing developed to quantify the homogeneity of the powder bed layers during spreading.

In this document, the flowability of five metal powders are investigated with an automated rotating drum method, whose dynamic cohesive index measurement is shown to establish a correlation with the spreadability of the powder during the layer deposition operation. Furthemore, the particle size distribution (PSD) and morphology of each powder is characterized before testing by static image analysis method (according to ISO 13322-1).

The general principle of the method is described in Figure 1.

2 Normative references

The following documents are referred to in the text in such a way that some or all of their content constitutes requirements of this document. For dated references, only the edition cited applies. For undated references, the latest edition of the referenced document (including any amendments) applies.

ISO/ASTM 52900, *Additive manufacturing — General principles — Fundamentals and vocabulary*

3 Terms and definitions

For the purposes of this document, the terms and definitions given in ISO/ASTM 52900 and the following apply.

ISO and IEC maintain terminological databases for use in standardization at the following addresses:

— ISO Online browsing platform: available at https://www.iso.org/obp

— IEC Electropedia: available at https://www.electropedia.org/

3.1
cohesiveness
physical powder behaviour relating to the degree to which the attractive forces between particles exceed the average particle mass

Note 1 to entry: Cohesive powders are qualified as powders where the attractive force between particles exceed the average particle mass

3.2
powder flowability
ability of a solid bulk material to flow

Note 1 to entry: Powder flowability is a function of multiple factors, and particularly powder size and distribution, see also ISO/ASTM 52907.

4 Designation

In this document, five powders described in Table 1 are used:

Table 1 — Designation of powders

Common designation	European spefication	Denomination used in this document
Scalmalloy®[1]	AlMgSc	AlMgSc_Std
Inconel®[2]	$NiCr_{22}Mo_9Nb$	$NiCr_{22}Mo_9Nb$_Std
$AlSi_7Mg$	$AlSi_7Mg$	$AlSi_7Mg$_Std
Titanium Fine	Ti_6Al_4V	Ti_6Al_4V_Fine
Inconel® Fine	$NiCr_{22}Mo_9Nb$	$NiCr_{22}Mo_9Nb$_Fine

5 Methodology

5.1 General principle

The general principle for comparing rotating drum measurements with powder spreading in a PBF-LB AM machine is described in Figure 1.

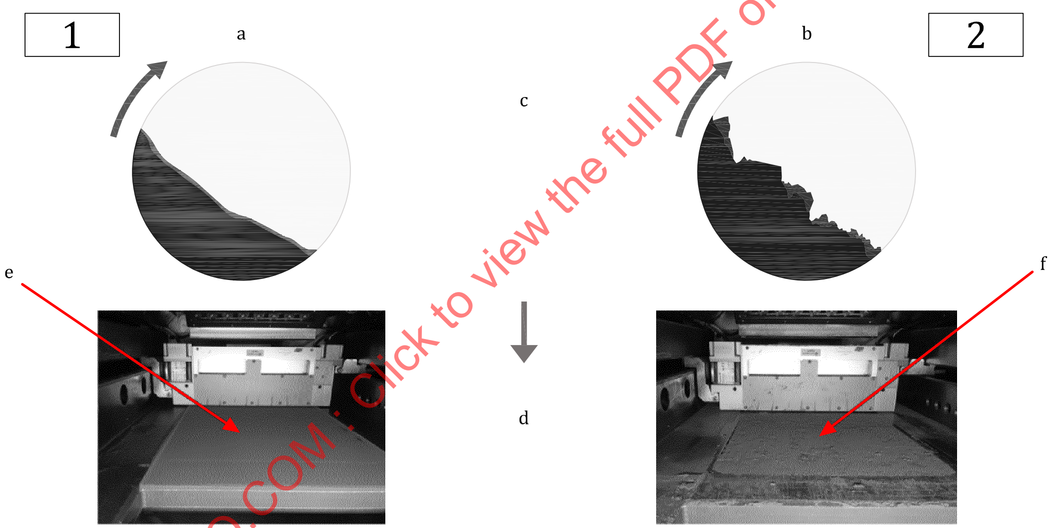

Key

1 $AlSi_7Mg$

2 $NiCr_{22}Mo_9Nb$ (Inconel® fine)

a Good.

b Bad.

c Rotating drum.

d PBF-LM machine.

e Regular layer.

f Irregular layer.

Figure 1 — General principle of comparing rotating drum measurements with powder spreading in a PBF-LB AM machine

1) Scalmalloy is an example of a suitable product available commercially. This information is given for the convenience of users of this document and does not constitute an endorsement by ISO of this product.

2) Inconel is an example of a suitable product available commercially. This information is given for the convenience of users of this document and does not constitute an endorsement by ISO of this product.

5.2 Powder selection

The recoating performance of the powders inside a PBF-LB AM machine is evaluated experimentally with in situ observation of layer homogeneity. Five metallic powders are selected for this study: two Nickel alloys ($NiCr_{22}Mo_9Nb$_Std and $NiCr_{22}Mo_9Nb$_Fine), two Aluminium alloys ($AlSi_7Mg$_Std and AlMgSc_Std) and one Titanium alloy (Ti_6Al_4V_Fine). Particle size distribution (PSD) is summarized in Table 2 and shape and morphology in Table 3.

Table 2 — Summary of the PSD (D10 and D90) of the five powders (volume)

Powder	D10 µm	D90 µm
AlMgSc_Std	26	66
$AlSi_7Mg$_Std	27	69
$NiCr_{22}Mo_9Nb$_Std	17	45
$NiCr_{22}Mo_9Nb$_Fine	6	27
Ti_6Al_4V_Fine	7	28

Table 3 — Shape and morphology comparison

Aspect ratio comparison				
Aspect ratio (number)	**Mean** µm	**P10** µm	**P50** µm	**P90** µm
AlMgSc_Std	79,7	62,5	81,6	93,8
$AlSi_7Mg$	76,6	58,4	78,7	91,8
$NiCr_{22}Mo_9Nb$_Std	81,9	63,5	85,3	94,6
$NiCr_{22}Mo_9Nb$_Fine	81,8	63,5	85,8	93,3
Ti_6Al_4V_Fine	79,7	60,9	82,9	92,8
Bluntness comparison				
Bluntness (number)	**Mean** µm	**P10** µm	**P50** µm	**P90** µm
AlMgSc_Std	74,6	54,0	74,6	95,1
$AlSi_7Mg$	75,5	57,1	75,5	93,8
$NiCr_{22}Mo_9Nb$_Std	84,3	67,9	86,7	97,2
$NiCr_{22}Mo_9Nb$_Fine	88,0	76,5	89,9	97,1
Ti_6Al_4V_Fine	85,0	70,2	87,4	96,5

Successive powder layers are deposited in the PBF-LB AM machine with no laser melting. Between each layer deposition, a picture of the powder layer is taken by a staring camera placed inside the AM machine. The pictures are then processed numerically to evaluate the layer homogeneity. Three powder spreading speeds are investigated: 30 mm/s, 80 mm/s and 160 mm/s to highlight their influence on the layer quality.

5.3 Layer homogeneity evaluation

The powder layer surface homogeneity is experimentally evaluated using a staring camera placed orthogonal to the powder bed. After each powder spreading operation, a picture is taken. For this experiment, the focus is made on metallic coater and 30 µm layer thickness only. For the same recoater speed, 15 layers are created and therefore, 15 pictures are taken as well. This methodology provides a quantitative and operator independent way to quantify the layer topography homogeneity.

The gathered pictures are then processed numerically to obtain "Interface Fluctuation", a measure of the inhomogeneity of the produced layers. The image processing analysis principle is as follow:

a) each picture is analysed separately. The picture size is 1 200 pixels × 1 200 pixels;

b) horizontal and vertical pixel intensity profiles are extracted at discrete positions of the picture [see Figure 2 a)];

c) an average "smooth" profile is computed for each position [see Figure 2 b)];

d) interface fluctuation is then computed based on the deviation around the averaged profile, and then averaged over all positions;

e) the process is repeated for all images, and the interface fluctuation is averaged over the whole set of pictures.

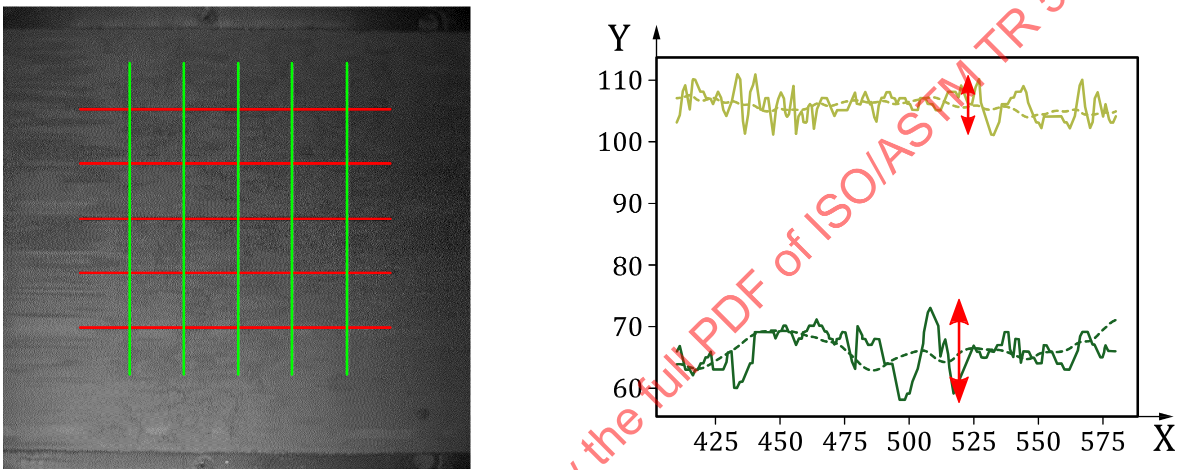

a) **Horizontal and vertical lines from which pixel intensity profiles are extracted**

b) **Pixel intensity profile (plain) and average profile (dashed) used to compute the interface fluctuation**

Key

X position along the line

Y pixel intensity (before normalisation)

---- AlSi$_7$Mg (top)

---- NiCr$_{22}$Mo$_9$Nb_Fine (bottom)

Figure 2 — In situ layer quality assessment

5.4 Rotating drum

Powder flowability is evaluated with a rotating drum method which allows an automated measurement.

A horizontal cylinder with transparent sidewalls called drum is filled with the sample of powder. The filling ratio of the drum can influence the flow of the powder and thus is kept constant to allow relevant comparison of the results.

The volume of the drum used in this study is 100 ml and the filling ratio is fixed as 50 %. Therefore, a 50 mL powder sample is used for the measurements.

The drum rotates around its axis at an angular velocity ranging from 2 r/min to 60 r/min. A CCD (charge-coupled device) camera takes snapshots at a framerate of 1 image per second for each angular velocity.

The air/powder interface is detected on each snapshot with an edge detection algorithm.

Afterwards, the average interface position and the fluctuations around this average position are computed. The number of snapshots taken influences the statistical relevance of the averaged interface. In this experiment and, based on previous studies[18], a value of 40 is chosen for each rotating speeds. This value is considered sufficient to guarantee accurate and reproducible measurements[27].

The number of revolutions performed during the measurement is dependant on the rotating speed. However, the rotating drum allows a continuous flow of material regardless of the angular position of the drum and number of revolutions, justifying the use of a fixed number of snapshots taken whatever the speed investigated. Then, for each rotating speed, the dynamic cohesive index σf is measured from the temporal fluctuations of the powder/air interface. The angle formed by the flow, commonly measured with rotating drum, is influenced by a wide set of parameters: the friction between the grains, the shape of the grains, the cohesive forces (van der Waals, electrostatic and capillary forces) between the grains.

On the opposite, the dynamic cohesive index σf is only related to the cohesive forces between the grains as highlighted in Reference [26]. A cohesive powder leads to an intermitted flow while a non-cohesive powder leads to a regular flow. Therefore, a dynamic cohesive index close to zero corresponds to a non-cohesive powder. When the powder cohesiveness increases, the dynamic cohesive index increases accordingly.

6 Results and discussion

6.1 Spreadability

The interface fluctuation, a measure of the layer homogeneity, obtained for the powders at different recoater speeds is presented in Figure 1.

In addition, a qualification of the layers spreadability is made according to the observations of the operator. These are summarized in Table 4.

Table 4 — Qualification of spreadability made by the operator during testing (based on visual observation)

Powder	Observation	Qualification remark
$AlSi_7Mg$_Std	Good spreading	Good
$NiCr_{22}Mo_9Nb$_Std	Good spreading	Good
AlMgSc_Std	Good spreading with rigid wriper. Seems to be speed dependant in case of spreading with silicon blade.	Medium
Ti_6Al_4V_Fine	Bad spreading/difficulties to obtain a uniform layer on the whole plate	Bad
$NiCr_{22}Mo_9Nb$_Fine	Bad spreading	Bad

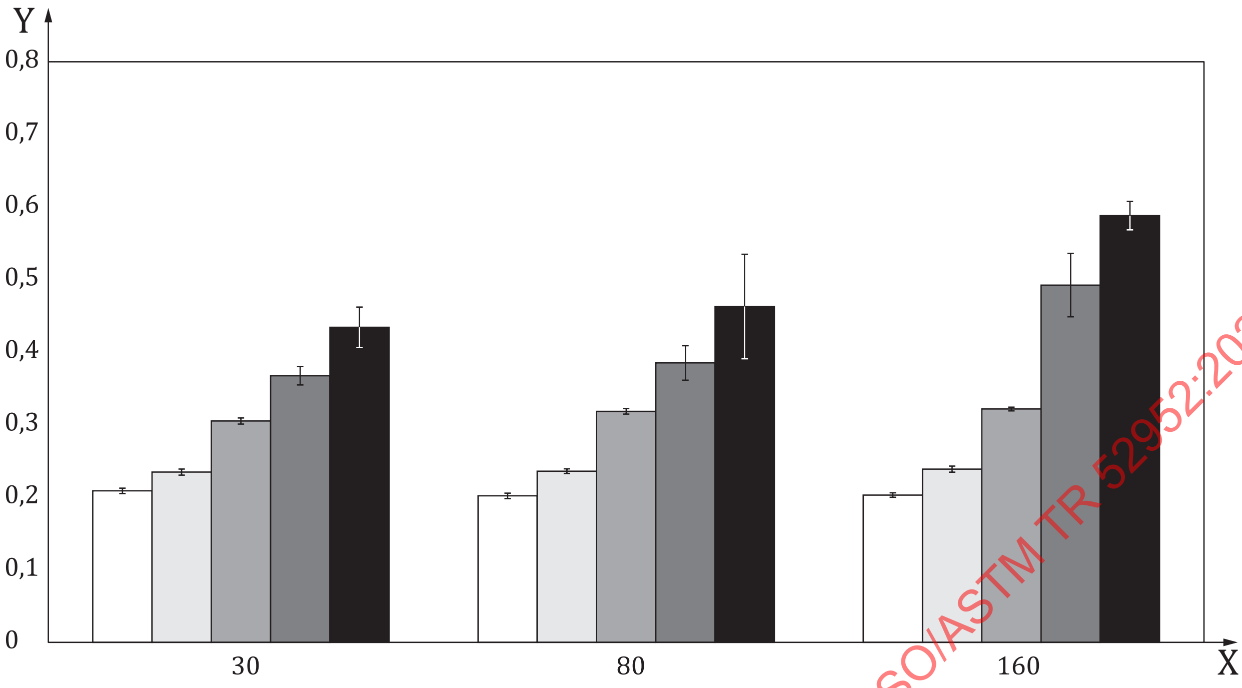

Key

X recoated speed (mm/s)

Y interface fluctuation

□ $NiCr_{22}Mo_9Nb$_Std

□ $AlSi_7Mg$_Std

□ AlMgSc_Std

□ $NiCr_{22}Mo_9Nb$_Fine

■ Ti_6Al_4V_Fine

NOTE The speed for powder spreading effect is noticeable for $NiCr_{22}Mo_9Nb$_Fine and Ti_6Al_4V_Fine.

Figure 3 — Interface fluctuations as a function of recoater speed (in mm/s)

Table 5 — Interface fluctuations (IF) as a function of recoater speed (in mm/s)

Interval of fluctuation vs. material										
Spreader speed	**$NiCr_{22}Mo_9Nb$_Std**		**$AlSi_7Mg$_Std**		**AlMgSc_Std**		**$NiCr_{22}Mo_9Nb$_Fine**		**Ti_6Al_4V_Fine**	
mm/s	**IF**	**Deviation**	**IF**	**Deviation**	**IF**	**Deviation**	**IF**	**Deviation**	**IF**	**Deviation**
30	0,21	0,004	0,23	0,004	0,30	0,004	0,37	0,013	0,43	0,028
80	0,20	0,004	0,24	0,003	0,32	0,004	0,38	0,024	0,46	0,072
160	0,20	0,003	0,24	0,004	0,32	0,003	0,49	0,044	0,59	0,020

$NiCr_{22}Mo_9Nb$_Std and $AlSi_7Mg$_Std show the lower interface fluctuation and, thus, are able to produce more homogeneous layers during the recoating. AlMgSc_Std exhibits a higher interface fluctuation; a consequence of the appearance of a parallel waves pattern is shown in Figure 4. The $NiCr_{22}Mo_9Nb$_Fine has the highest interface fluctuation and thus produces the less homogeneous layers among the tested powders [see Figure 4 b)]. This could be attributed to the smaller particle sizes compared to the $NiCr_{22}Mo_9Nb$_Std.

Indeed these two $NiCr_{22}Mo_9Nb$ powders have very close morphological criteria, see Figure 4. So, the difference of behaviour between these two powders seems to be due mainly to the effect related to the size of the grains.

Furthermore, the smaller the particles the higher the influence of the cohesive interactions lying between the particles composing the powders.

For $NiCr_{22}Mo_9Nb$_Fine and Ti_6Al_4V_Fine, the interface fluctuation with increasing recoater speed is observed. This indicates a degradation of the layer homogeneity when the recoating process is speed up. However, increasing the speed for powder spreading is interesting in order to reduce the printing duration. Therefore, this highlights the existence of an optimal speed for spreading powder, specific for each powder, at which the time spent on spreading powder is minimized while still guaranteeing sufficiently homogeneous layers. Moreover, the decrease of spreading performance when the powder is submitted to a higher shear stress may indicate that the rheology of the powder is also a key parameter for spreadability.

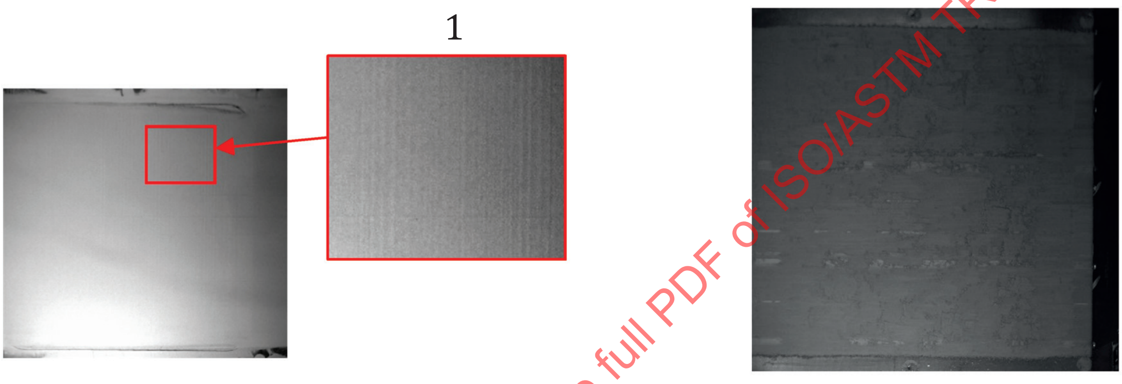

a) AlMgSc_Std   b) $NiCr_{22}Mo_9Nb$_Fine at 30 mm/s

Key

1 parallel waves

Figure 4 — Example of in-situ photography

6.2 Rotating drum analysis

6.2.1 Experimental protocol

For an experiment with the rotating drum, powders are poured inside the measuring cell just after the box opening. The quantity of powder used is 50 ml. Every powder is analysed under ambient conditions (35 % RH and 23 °C). Rotating drum velocities are investigated from 2 r/min to 60 r/min. For each velocity, 40 pictures are taken to assess accuracy and repeatability of the measurement. Three independent tests are performed on unused powder to evaluate the reproducibility. Error bars depict the standard deviation with respect to the average value.

6.2.2 Experimental results

Figure 5 shows the dynamic cohesive index as a function of the rotating drum speed. The dynamic cohesive index is linked to the fluctuations of the powder/air interface.

The recoater speed can be approximated to tangential velocity seen by the powder in the drum as follows: rotational speed multiplied by radius [r/min (rad/sec) × r]. For ease of comparison, the three recoater speeds used in the PBF-LB AM machine measurements are thus indicated.

The five powders can be classified according to their dynamic cohesive index. At low rotating speed, $AlSi_7Mg$_Std has the lowest dynamic cohesive index, followed by $NiCr_{22}Mo_9Nb$_Std and AlMgSc_

Std. Over the explored velocity range, $NiCr_{22}Mo_9Nb$_Fine and Ti_6Al_4V_Fine exhibit the high dynamic cohesive index.

According to the PSD and morphology analyses done of each powder, when comparing $NiCr_{22}Mo_9Nb$_Std with $NiCr_{22}Mo_9Nb$_Fine, it can be seen that these powders have very close morphological criteria but very different PSD. In this case, the predominance of the impact of cohesive forces on the interface fluctuation and also on cohesive index can be supposed.

On $NiCr_{22}Mo_9Nb$_Fine and Ti_6Al_4V_Fine powders, a higher cohesive index associated with a bad spreadability can be noticed.

Upon increasing the rotating speed, the powder is submitted to higher shear stress allowing to investigate its rheological behaviour. All the powders exhibit a shear-thickening behaviour except for Ti_6Al_4V_Fine, i.e. an increase of dynamic cohesive index with increasing rotating speed, stronger for rotating speed above 40 r/min. Therefore, the flowability is expected to decrease at higher shear stress. AlSi7Mg_Std and AlMgSc_Std powders are particularly affected compared to $NiCr_{22}Mo_9Nb$_Std, leading to a significant difference at 60 r/min. Unfortunately, this study does not deal with blade speeds of this magnitude in order to clearly highlight this effect on interval of fluctuation.

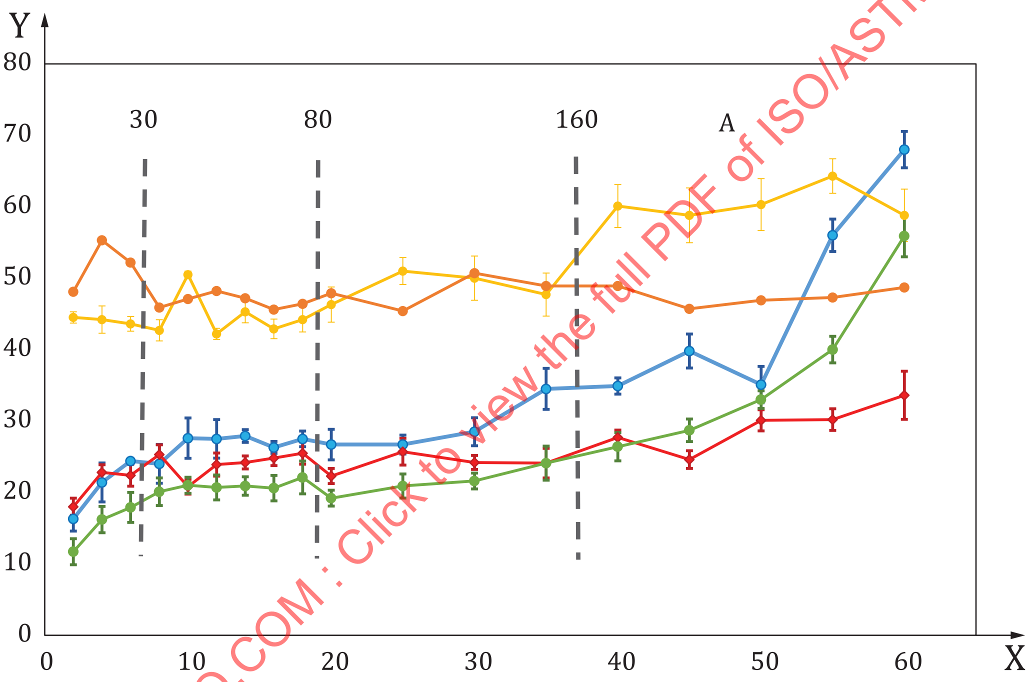

Key

X rotating speed (r/min)

Y dynamic cohesive index

- $NiCr_{22}Mo_9Nb$_Std
- $AlSi_7Mg$_Std
- AlMgSc_Std
- $NiCr_{22}Mo_9Nb$_Fine
- Ti_6Al_4V_Fine

NOTE Concerning Ti_6Al_4V_Fine, only one drum measurement was done due to low quantity of powder available, which explains the absence of an error bar in the above graph.

Figure 5 — Dynamic cohesive index versus rotating drum speed

6.3 Discussion

The spreadability investigation highlights major differences in the quality of the produced layers between the tested powders. The flowability of the powder is expected to play a key role in its ability to spread as uniform and homogeneous layers. Therefore, the powders flowability is evaluated in a rotating drum. Results gathered from both analyses are summarized in Figure 6 and Figure 7.

In this discussion, material families are first compared in order to assume that the interaction between blade regarding powder layer has the same effect on the fluctuation interval measurements related to the in-situ spreading condition (e.g.: tribocharging, etc.) and therefore can be ignored.

Interestingly, the $NiCr_{22}Mo_9Nb$_Fine which produces the less homogeneous layers also exhibits higher cohesive index compared to $NiCr_{22}Mo_9Nb$_Std. This is also observed when comparing AlMgSc_Std to $AlSi_7Mg$_Std by measuring the dynamic cohesive index and their ability to produce homogeneous layers in the AM machine.

Moreover for $NiCr_{22}Mo_9Nb$_Fine and Ti_6Al_4V_Fine, the increase of dynamic cohesive index observed in the rotating drum for high rotating speeds is correlated with an increase of interface fluctuation and thus a decrease of layer quality.

However, $NiCr_{22}Mo_9Nb$_Std does not follow the above observations.

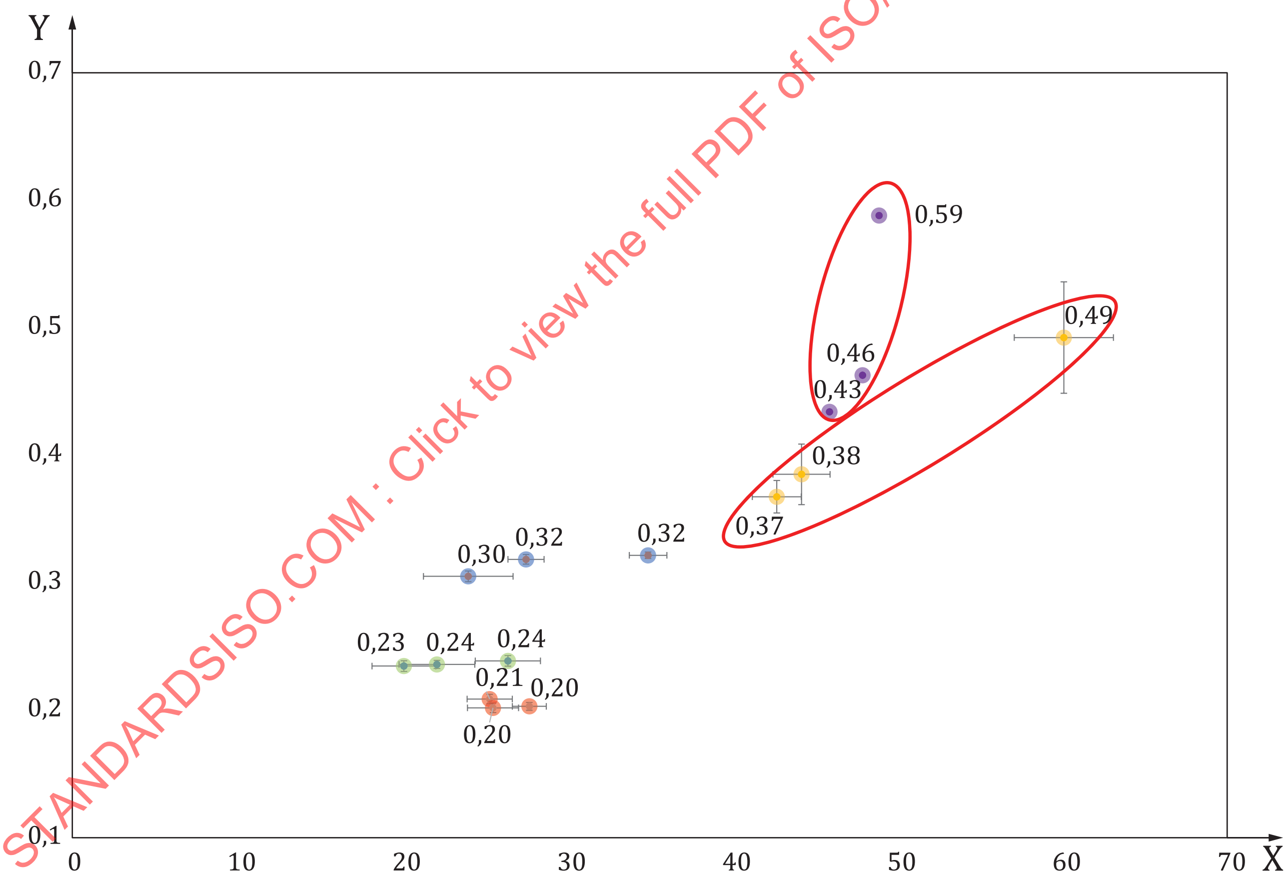

Key

X	dynamic cohesive index
Y	interface fluctuation
●	$NiCr_{22}Mo_9Nb$_Std
●	$AlSi_7Mg$_Std
●	AlMgSc_Std
●	$NiCr_{22}Mo_9Nb$_Fine
●	Ti_6Al_4V_Fine

error bar

Figure 6 — Interface fluctuations versus dynamic cohesive index of all powders

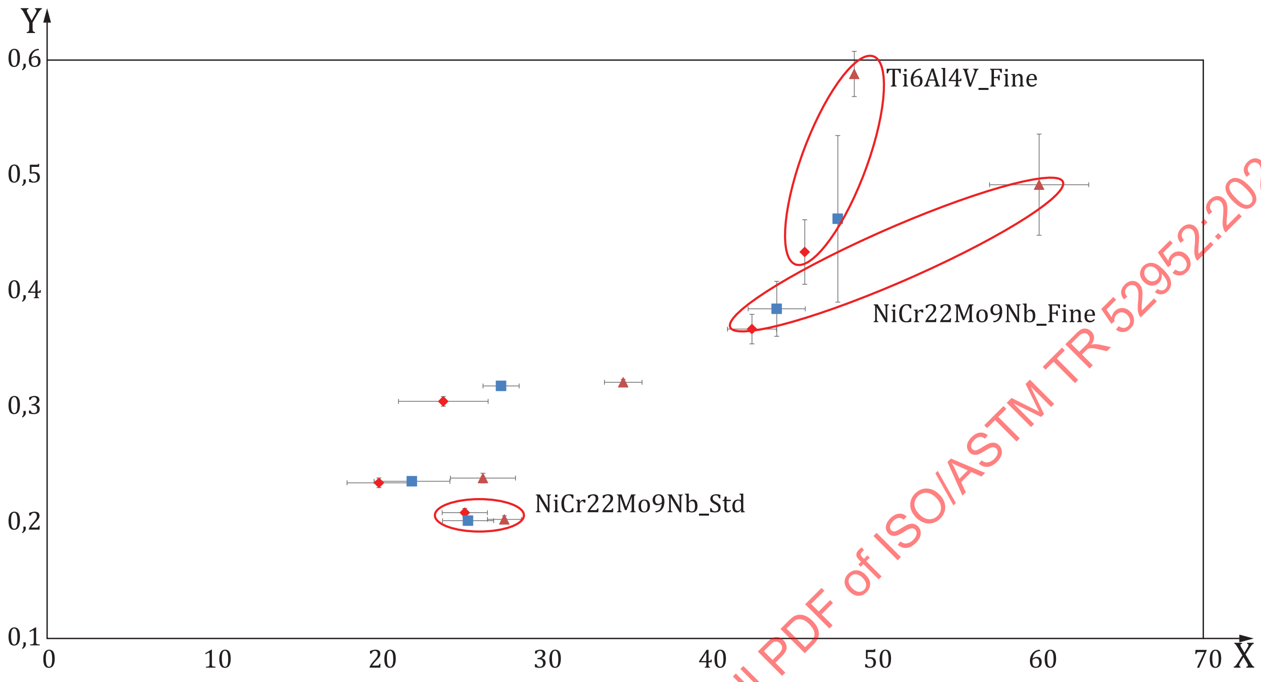

Key

X dynamic cohesive index

Y interface fluctuations

◆ 30 mm/s

■ 80 mm/s

▲ 160 mm/s

error bar

Figure 7 — Interface fluctuations as a function of the dynamic cohesive index and spreading speed

Last, based on the qualification of the layers made by the operator (see Figure 4), the powders presenting a bad spreadability have a value of cohesive index higher than 40 while the powders presenting a good spreadability are under a cohesive index of 30.

7 Conclusions

In this document, the ability of five metal powders to produce homogeneous layers during recoating is evaluated with the use of image processing of pictures of the powder bed and by taking into account the operator observation. A new measure, the interface fluctuation, is introduced as a measure of the powder layer homogeneity in addition to the operator observation. All powders materials tested exhibits measurable differences in their interface fluctuation.

The powder flowability and rheology is evaluated with a rotating drum and quantified with the dynamic cohesive index measurement. Significant differences are observed in cohesiveness.

Powder characterization with a rotating drum can provide a useful information on powder behaviour that can be used to estimate its spreadability.

Indeed, the powders presenting a bad spreadability have a value of cohesive index higher than 40 while the powders presenting a good spreadability are under a cohesive index of 30.

Furthermore, one powder among the five tested exhibits a clear degradation of layer quality at higher recoater speeds, indicating an influence of the powder properties at different speeds (rheology) on the spreadability.

For this specific powder ($NiCr_{22}Mo_9Nb$_Fine), a correlation between the fluctuation interface and the cohesion index is noticed. On the other hand, no correlation is noticed between the fluctuation interface and the cohesion index of $NiCr_{22}Mo_9Nb$_Std.

8 Additional data

In order to strengthen the results of this study showing the pertinence of the drum measurement to evaluate the suitability of a powder to be spread in an AM machine, other data were collected.

In the measurements provided in Table 6 and Figure 8, results are obtained for $NiCr_{19}Fe_{19}Nb_5Mo_3$ (commonly named as Inconel®[3] 718) with another rotating drum system.

a) $NiCr_{19}Fe_{19}Nb_5Mo_3$ recycled R54: good flowability

b) $NiCr_{19}Fe_{19}Nb_5Mo_3$ fresh: intermediate flowability

c) $NiCr_{19}Fe_{19}Nb_5Mo_3$ moistened powder mixture: intermediate flowability

Figure 8 — Results obtained with another rotating drum

3) Inconel is an example of a suitable product available commercially. This information is given for the convenience of users of this document and does not constitute an endorsement by ISO of this product.

